

Proton Excitations in $^{49}\text{V}^\dagger$

D. J. PULLEN AND BARUCH ROSNER*

Department of Physics, University of Pennsylvania, Philadelphia, Pennsylvania

AND

OLE HANSEN

The Niels Bohr Institute, University of Copenhagen, Denmark

(Received 5 September 1967)

The reaction $^{48}\text{Ti}(^3\text{He},d)^{49}\text{V}$ has been studied at around 17-MeV incident energy with an over-all resolution of 20 keV. Ninety-four levels were observed up to 8.7-MeV excitation, and the corresponding deuteron angular distributions were recorded in the angular interval 7.5° to 40° . Spectroscopic information has been extracted for 26 of the stronger transitions by means of a distorted-wave analysis of the differential cross sections. The results are compared to nuclear-structure-model predictions.

I. INTRODUCTION

IN the present paper the results of an investigation of the $^{48}\text{Ti}(^3\text{He},d)^{49}\text{V}$ reaction are reported. This experiment forms part of a systematic study of proton states in the $Z=23$ nuclei by $(^3\text{He},d)$ proton capture on titanium targets. The results obtained for ^{47}V have already been published.¹

II. EXPERIMENTAL TECHNIQUES AND RESULTS

Self-supporting metal foils² of 99% enriched ^{48}Ti were bombarded by ^3He ions accelerated to energies up to 17 MeV in the University of Pennsylvania tandem electrostatic generator. The reaction deuterons were momentum-analyzed in a broad-range magnetic spectrograph and detected in nuclear emulsions. A deuteron spectrum obtained at a reaction angle of 25° is shown in Fig. 1. The excitation energies given in column 3 of Table I were obtained from measurements at 16.4-MeV incident energy and are the means of values obtained at three different angles with an energy resolution better than 20 keV. The excitation energies determined by Brown *et al.*,³ using the $^{52}\text{Cr}(p,\alpha)^{49}\text{V}$ reaction at $E_p=11$ and 12 MeV, are shown in column 2 of Table I. It is evident that a number of states in ^{49}V have been missed in the present experiment, presumably indicating a greater selectivity of the $(^3\text{He},d)$ reaction over the (p,α) reaction.

Angular distributions were measured at 17.0-MeV incident energy for 28 of the more intense or isolated deuteron groups, using a somewhat thicker target which resulted in an energy resolution of about 45 keV. The angular distributions are displayed in Figs. 2 and 3 and cover an angular interval of 7.5° to 40° in the laboratory

system. The cross-section units in these figures are arbitrary, and the different distributions are not shown on the true relative scale. An absolute cross-section scale was established for the 17-MeV data to within $\pm 30\%$ by a differential weighing procedure combined with a measurement of the relative mass composition of the target. The latter was obtained from elastic-scattering yields using a 6-MeV $^3\text{He}^+$ beam. The maximum differential cross section for each of the stripping-type angular distributions is quoted in column 4 of Table I.

III. DISTORTED-WAVE ANALYSIS

The spectroscopic strengths, defined as $(2j+1)S(j)$, where j is the angular momentum of the transferred proton and $S(j)$ is the spectroscopic factor, are given in column 6 of Table I. Since the target spin in the present case is zero, the final-state spin is also equal to j . The strengths were extracted by comparing the measured maximum cross sections with distorted-wave (DW) calculations, using the relation

$$(\frac{d\sigma}{d\Omega})_{\text{exp}} = 4.4(2j+1)S(j)\sigma_{\text{DW}}, \quad (1)$$

as suggested by Bassel.⁴ The optical-model parameter sets used in the DW calculations were those labelled *BA1* (^3He channel), *PE1* (d channel) and *PR0* (bound state) in Table II.

The predicted cross sections were found to be rather insensitive to the application of a lower cutoff on the radial integrals for values between 0 and 4.3 fm. For example, the change in the calculated maximum cross section for the ground-state transition was less than 4% over this range. Omission of the spin-orbit coupling in the deuteron channel, or changing from the *PE1* to the *PE2* set of deuteron potentials (see Table II), also produced effects which were less than 4% on the DW cross sections. Changing the ^3He potential from the 180-MeV family (*BA1*) to the 130-MeV family (*BA2*) resulted in a 16% increase in the maximum cross section for the ground-state transition. The angular-distribution

[†] Work supported by the National Science Foundation under a contract with the University of Pennsylvania.

* On leave of absence from the Department of Physics, Technion-Israel Institute of Technology, Haifa, Israel.

¹ Baruch Rosner and D. J. Pullen, *Phys. Rev.* **162**, 1048 (1967).

² The enriched material was obtained from Oak Ridge National Laboratory, Isotopes Sales Division.

³ G. Brown, A. MacGregor, and R. Middleton, *Nucl. Phys.* **77**, 385 (1966).

⁴ R. H. Bassel, *Phys. Rev.* **149**, 791 (1966).

TABLE I. Results from the $^{48}\text{Ti}(^3\text{He},d)^{49}\text{V}$ reaction.

Deuteron group	E_x (keV) Ref. a Present ^b	$d\sigma/dw$ max ^c (mb/sr)	l_p	Spectroscopic strength ^d	Shell-model assignment ^e	Deuteron group	E_x (keV) Ref. a Present ^b	$d\sigma/dw$ max ^c (mb/sr)	l_p	Spectroscopic strength ^d	Shell-model assignment ^e	
0	0	0	1.3	3	2.5	$1f_{7/2}$	42	5962	...			
1	91	83	0.06	...			43	6000	0.74	1	0.07	$2p$
2	152	152	0.65	1	0.07	$2p$	44	6038	...			
3	749	751	0.40	2	0.41	$1d_{3/2}$	45	6095	...			
4	1025	1036			46	6147	...			
5	1140	1149			47	6181	...			
	1157				48	6212	0.72	1	0.07	$2p$
	1521				49	6252	...			
	1607				50	6327	0.99	1	0.11	$2p$
	1647				51	6363	...			
6	1664	1663	3.80	1	0.38	$2p$	52	6416	...			
	1999				53	6459	...			
7	2184	2185	0.42	3	0.53	$1f$	54	6507	...			
	2240				55	6541	...			
8	2266	2265	3.6	1	0.35	$2p$	56	6590	...			
9	2312	2307	6.8	1	0.67	$2p$	57	6654	...			
	2357				58	6683	...			
10	2395	2388			59	6711	...			
	2413				60	6816	...			
	2679				61	6856	...			
	2796				62	6892	...			
11	2820	2820	0.39	3	0.43	$1f$	63	6943	...			
12		3141			64	6978	...			
13		3401	0.19	...			65	7054	...			
14		3464			66	7099	...			
15		3688			67	7137	1.0	...		
16		3763 ^f	0.48	{(1) (3)}	0.05	$2p$	68	7240	...			
17		3932	1.9	1	0.16	$1f$	69	7290	...			
18		4018	0.36	1	0.03	$2p$	70	7365	...			
19		4145			71	7430	0.87	(1)	unbound ($2p$)	
20		4235			72	7478	...			
21		4265	0.80	{1 1}	0.07	$2p$	73	7554	...			
22		4385	0.31	1	0.02	$2p$	74	7605	...			
23		4448			75	7645	...			
24		4511	1.4	1	0.13	$2p$	76	7783	3.9	(1)	unbound $2p_{3/2}, T=\frac{5}{2}$	
25		4600			77	7850	...			
26		4657	0.98	3	0.75	$1f$	78	7896	...			
27		4862	1.5	1	0.13	$2p$	79	7947	...			
28		4894			80	7999	...			
29		4954	0.22	1	0.02	$2p$	81	8079	...			
30		5010			82	8111	1.6	(1)	unbound $2p_{1/2}, T=\frac{5}{2}$	
31		5064	0.36	1	0.03	$2p$	83	8192	...			
32		5218	1.1	1	0.09	$2p$	84	8246	...			
33		5251			85	8277	...			
34		5367			86	8326	...			
35		5392			87	8371	...			
36		5594			88	8405	...			
37		5687			89	8444	...			
38		5719			90	8491	...			
39		5761			91	8591	...			
40		5836			92	8665	...			
41		5899			93	8686	...			

^a G. Brown, A. MacGregor, and R. Middleton, Nucl. Phys. **77**, 385 (1966).

^b From 0 to 3 MeV the uncertainty in the excitation energy (E_x) is ± 10 keV. Between 3 and 6 MeV the uncertainty is ± 20 keV and above 6 MeV it is ± 30 keV.

^c The uncertainty in the cross-section scale was estimated to be $\pm 30\%$.

^d The strength is $(2j+1)S(j)$, where j is the transferred spin and S is the spectroscopic factor in a formalism without isospin. If the isospin is introduced, then $S(j) = (2j+1)T_{\frac{1}{2}}^2 S(j, T)$. Unless otherwise stated, it was assumed that $j=l+\frac{1}{2}$. See also Table III and text.

^e When no isospin is stated, $T=\frac{1}{2}$. The shell-model assignments were used in the DW analysis and were made on the basis of the assigned l values.

^f A doublet.

shapes for these two ^3He potentials also differed near the secondary maximum, and the $BA2$ potential gave a somewhat better fit to the data. Bock *et al.*⁵ have found a ^3He potential ($HE1$ of Table II) which fits elastic scattering from Cr but which has a real depth in between those of the $BA1$ and $BA2$ potentials. This

⁵ R. Bock, P. David, H. Duhm, H. Hefele, U. Lynen, and R. Stock, Nucl. Phys. **A92**, 539 (1967).

potential was found to give $(^3\text{He},d)$ cross sections which were within 2% of the $BA1$ cross sections. The Q -value and l -value dependence of the DW cross sections were quite similar for all potentials investigated.

The bound-state wave function should be computed with a spin-orbit term in the potential; therefore, a knowledge of the final-state spin j is required. Since the experiment determines the orbital angular momentum l

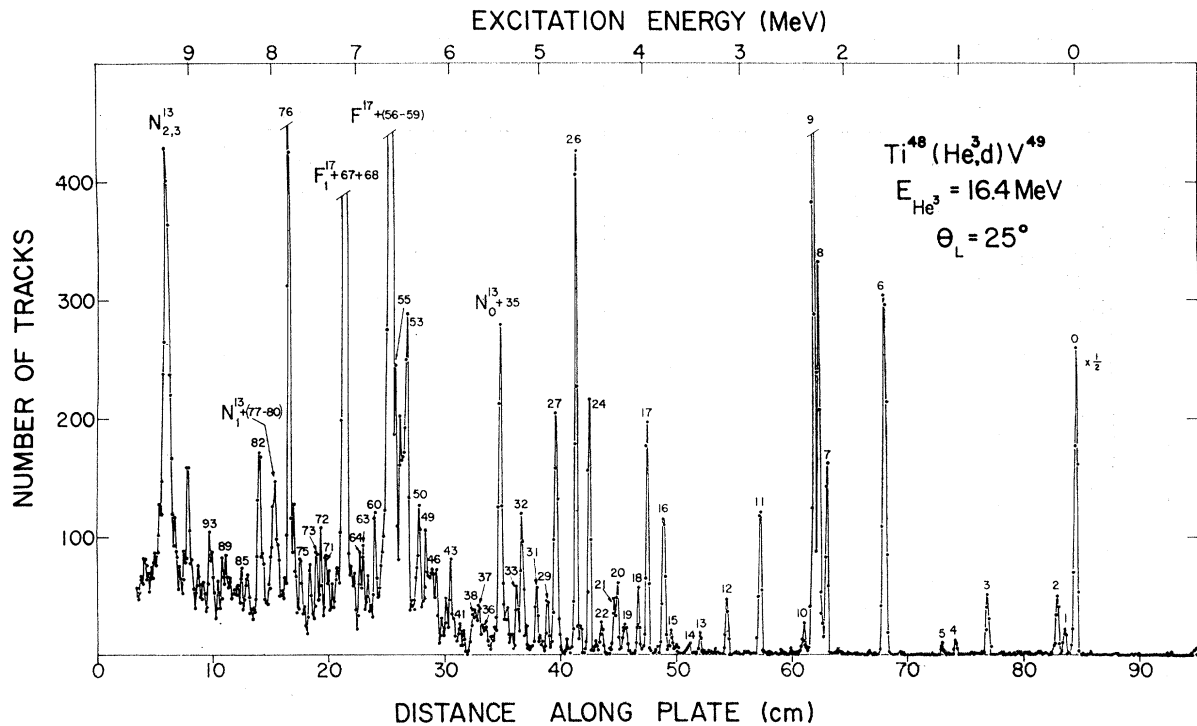


FIG. 1. Deuteron spectrum from the $^{48}\text{Ti}(^3\text{He},d)^{49}\text{V}$ reaction at 16.4 MeV and $\Theta_{\text{lab}} = 25^\circ$. The number of deuterons counted in 1.0-mm-wide strips across the exposed area of the photographic emulsion is plotted versus distance along the plate. The spectrograph calibration furnished the corresponding magnetic rigidities which, via the Q -value equation, lead to the excitation energy scale shown above the spectrum.

rather than the value of j , it has been assumed, unless otherwise stated, that $j = l + \frac{1}{2}$ in the evaluation of the bound-state wave function. A spin-orbit strength of 25 times the Thomas value was employed. In Table III, the calculated values of the ratio $\sigma_{\text{DW}}(j = l + \frac{1}{2}) / \sigma_{\text{DW}}(j = l - \frac{1}{2})$ are presented for several Q values and for $l = 1$ and $l = 3$. The procedure employed in the analysis will lead to an underestimation of the observed $1f_{5/2}$ and $2p_{1/2}$ spectroscopic strengths.

IV. SUM-RULE ANALYSIS

The $^{48}\text{Ti}(d,^3\text{He})$ reaction study by Yntema and Satchler⁶ shows that the $2p$ admixture in the proton part of the ^{48}Ti ground state is small. The present data indicate about 0.4 holes in the $1d_{3/2}$ proton orbital in the ground state. The (d,p) and (p,d) neutron-transfer reactions on ^{48}Ti also disclose little $1d_{3/2}$ and $2s_{1/2}$ core excitations,⁷ no $1f_{5/2}$ admixture, but some $2p_{3/2}$ admix-

TABLE II. Optical-model potentials.^a

Particle	Label	V	r_0	a	W	W'	r_0'	a'	V_{so}	r_{0c}
^3He	BA1 ^b	177.8	1.14	0.723	25.72	0	1.548	0.80	0	1.40
^3He	BA2 ^c	139	1.08	0.80	12.3	0	1.743	0.721	0	1.40
^3He	HE1 ^d	165	1.14	0.723	20.2	0	1.60	0.81	5	1.30
d	PE1 ^b	112	0.974	0.912	0	73.2	1.439	0.60	6	1.30
d	PE2 ^e	89.8	1.15	0.81	0	73.6	1.34	0.68	0	1.30
p	PRO ^f	Ref. f	1.25	0.65	0	0	0	0	Ref. f	1.25

^a The potentials for ^3He and d were of the form

$$V(r) = -V(1 + \exp x)^{-1} - i[W - W'(d/dx)](1 + \exp x)^{-1} + V_{so}(\hbar/M\pi c)^2(1/r)(d/dr)(1 + \exp x)^{-1} \cdot \sigma + V_c(r, r_c),$$

with

$$x = (r - r_0 A^{1/3})/a, \quad x' = (r - r_0' A^{1/3})/a', \quad \text{and} \quad r_c = r_{0c} A^{1/3}.$$

V_c is the Coulomb potential. V , W , W' , and V_{so} are given in MeV and the geometrical parameters in fm.

^b Used in Ref. 1; and given by Bassel (private communication).

^c See Ref. 4.

^d See Ref. 5.

^e C. M. Perey and F. G. Perey, Phys. Rev. **132**, 755 (1963); **152**, 923 (1966).

^f The spin-orbit part of the potential was proportional to V and its strength was 25 times the Thomas value. If the final-state spin was not known, it was assumed that $j = l + \frac{1}{2}$. The depth V of the potential was chosen so that the proton received a binding energy equal to $Q(^3\text{He}, d) + 5.49$ MeV.

⁶ J. L. Yntema and G. R. Satchler, Phys. Rev. **134**, B976 (1964).

⁷ P. D. Barnes, J. R. Comfort, C. K. Bockelman, O. Hansen, and A. Sperduto, Phys. Rev. **159**, 920 (1967).

TABLE III. Ratio of DW maximum cross sections for $j=l+\frac{1}{2}$ and $j=l-\frac{1}{2}$. A spin-orbit coupling of 25 times the Thomas value was used together with the potentials BA1 and PE1 of Table II [$\sigma_{\text{DW}}(j=l+\frac{1}{2})/\sigma_{\text{DW}}(j=l-\frac{1}{2})$].

Q (MeV)	$l=1$	$l=3$
2	1.2	1.8
0	1.1	1.7
-2	1.1	1.6
-4	1.1	1.6

ture.⁸ The $1f_{7/2}$ proton capture strength is therefore expected to be about 5.5 and the total $1f$ strength to be about 11.5. The $2p$ strength should be close to 6. In comparison, the total $1f$ and $2p$ strengths found in the present work are only 4.3 and 2.5, respectively. However, since the $T=\frac{5}{2}$ states (except the ground-state analog) are unbound in ^{49}V and transitions to unbound levels have not been analyzed, perhaps a fairer comparison may be had between experiment and theory by subtracting from the above estimates the $T=\frac{5}{2}$ sum-rule strength, as determined from the formula of French

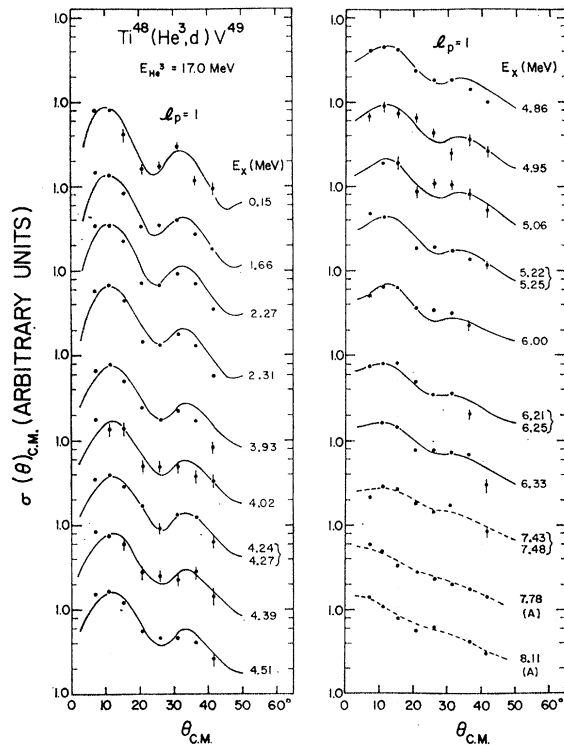


FIG. 2. Angular distributions of $l=1$ character. The experimental data are indicated by filled circles together with representative errors. The different distributions are plotted off scale, the true cross-section scale being given in Table I. The full curves are from distorted-wave calculations which are described in the text. The dashed curves were drawn through the experimental points and have no theoretical significance.

⁸ E. Kashy and T. W. Conlon, Phys. Rev. **135**, B389 (1964); R. Sherr, B. Bayman, E. Rost, M. Rickey, and C. G. Hoot, *ibid.* **139**, B1272 (1965).

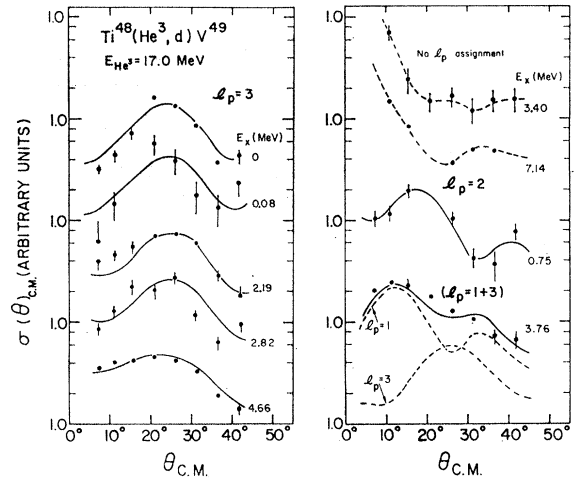


FIG. 3. Angular distributions of $l=3$ character (left) and $l=2$ or mixed $l=1+3$ character (right). The 0.08-MeV transition is probably of a nonstripping type as discussed in the text. See also caption of Fig. 2.

and MacFarlane.⁹ Assuming for the ^{48}Ti ground state a pure $(f_{7/2})^{-2}$ neutron configuration, which is consistent with experiment apart from the small $2p_{3/2}$ admixture, the $T=\frac{3}{2}$ strengths are approximately $10(1f)$ and $4.8(2p)$. It is clear, therefore, that the experimental strengths are substantially smaller than the expected values. Furthermore, the discrepancies cannot be explained entirely by the $j=l+\frac{1}{2}$ assumption underlying the DW analysis. Such a discrepancy may be explained in an *ad hoc* fashion in several ways: the missing strength could be distributed over many weak transitions, the cross-section scale could be in error, or the normalization constant in Eq. (1) may be too large. However, it is not possible on the basis of the present experiment alone to arrive at a definite conclusion regarding this problem.

V. DISCUSSION

A. Comparison with Shell-Model Calculations

Extensive shell-model calculations relevant to the structure of ^{49}V have been reported by McCullen, Bay-

TABLE IV. Coulomb energies. The Coulomb energy was calculated as $\Delta E_c = M(Z+1, N) + E_x(Z+1, N) - M(Z, N+1) - E_x(Z, N+1) + M(0, 1) - M(1, 0)$, where (Z, N) designates the target nucleus for the transfer reactions involved (^{48}Ti here) and M is a ground-state mass.^a

^{49}V E_x (keV)	l_p	^{48}Ti E_x (keV)	l_n	j^π	ΔE_c
7783	(1)	1384	1	$\frac{3}{2}^-$	7788 ± 30
8111	(1)	1724	1	$\frac{1}{2}^-$	7776 ± 30

^a The masses were taken from J. Mattauch *et al.*, Nucl. Phys. **67**, 1 (1965); the $^{48}\text{Ti}(d, p)$ data were from Ref. 7.

⁹ J. B. French and M. H. MacFarlane, Nucl. Phys. **26**, 168 (1961).

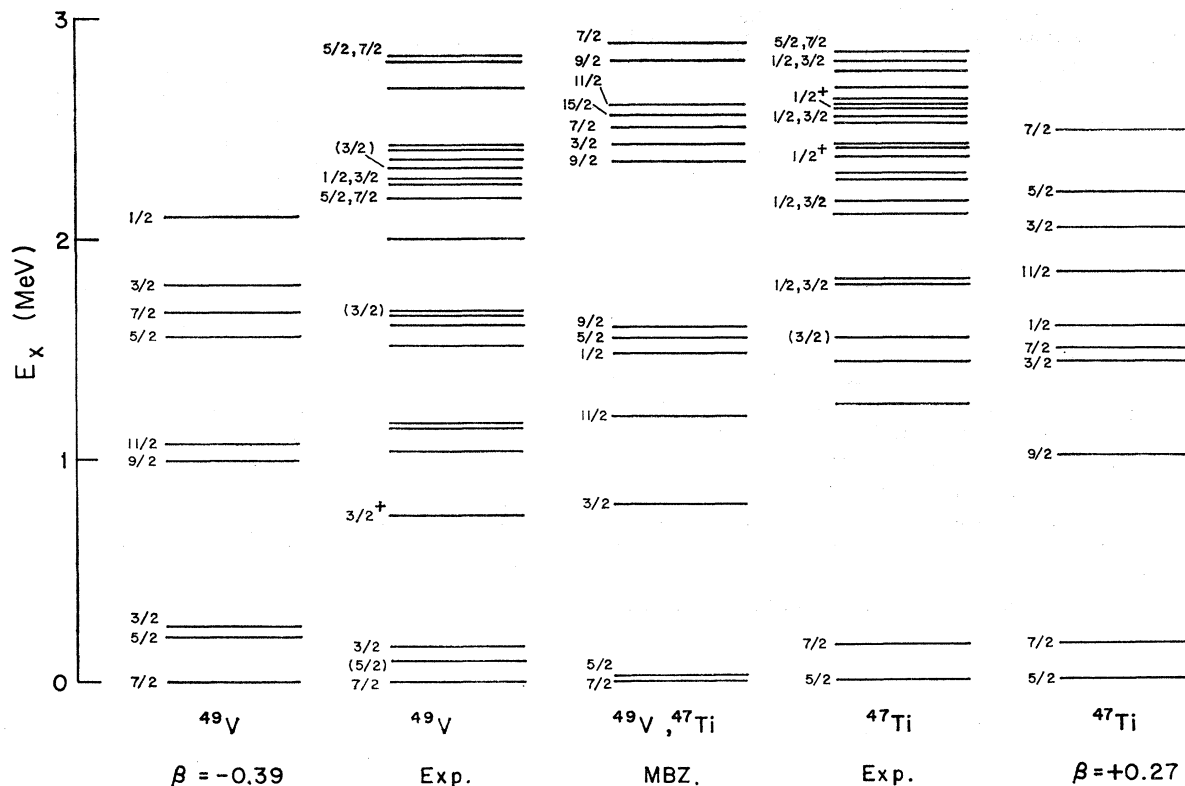


FIG. 4. Comparison of experimental and theoretical level schemes for ^{47}Ti and ^{49}V . From left to right are shown the ^{49}V level scheme of Malik and Scholz (Ref. 11) for a deformation of $\beta = -0.39$, the experimental ^{49}V level scheme (Table I), the $(f_{7/2})$ -model level scheme of Ref. 10, the experimental ^{47}Ti scheme (Ref. 7), and, finally, the ^{47}Ti level diagram from Ref. 11, assuming a deformation of $\beta = +0.27$.

man, and Zamick¹⁰ (MBZ) and by Malik and Scholz.¹¹ The MBZ model is based on pure $1f_{7/2}$ configurations, whereas the calculations of Malik and Scholz take into account the mixing of higher shell-model orbits by employing the aligned coupling scheme with Coriolis coupling. Auerbach¹² has also treated configuration mixing in the case of $N=28$ nuclei by starting from a spherical j - j coupling scheme.

A simple feature of the MBZ model is the existence of cross-conjugate symmetry, i.e., the identity of the $\pi(f_{7/2})^n \nu(f_{7/2})^{-m}$ and the $\pi(f_{7/2})^{-m} \nu(f_{7/2})^n$ configurations. This symmetry is destroyed when higher configurations mix in. Thus, in the MBZ model ^{47}Ti and ^{49}V are identical, and since ^{48}Ti is self-cross-conjugate, it follows that the $f_{7/2}$ proton capture and neutron pickup strength functions from a ^{48}Ti target should be identical. In ^{47}Ti and ^{49}V , $\frac{7}{2}^-$ states are predicted at 0-, 2.50-, and 2.87-MeV excitation with spectroscopic strengths of 4.8, 0.14, and 0.55, respectively. In the present work, $l=3$ transitions are observed to ^{49}V states at 0, 2.19, and 2.82 MeV, having strengths of 2.5, 0.5, and 0.4, respectively. In ^{47}Ti , $l=3$ transitions to states at 0.16 and 2.8 MeV have been observed in the $^{48}\text{Ti}(p,d)$ reaction⁸

with relative strengths of 4.6 and 0.9, respectively. Thus, the cross-conjugate symmetry is not observed experimentally for the $\frac{7}{2}^-$ states.

The MBZ model also predicts low-lying $\frac{5}{2}^-$ and $\frac{3}{2}^-$ states at 0 and 0.8 MeV, respectively, in ^{49}V and ^{47}Ti . The $\frac{5}{2}^-$ state is found at 0 MeV in ^{47}Ti and (presumably) at 83 keV in ^{49}V , and the spectroscopic strengths are small. These transitions should be of second order or nondirect type as observed in the $^{46}\text{Ti}(d,p)^{47}\text{Ti}$ reaction.¹³ The present angular-distribution data, extending only to 40° , are not sufficient to demonstrate whether the transition to the 83-keV state in ^{49}V is, indeed, of second-order type. The lowest candidate for a $\frac{3}{2}^-$ assignment in ^{49}V is the 152-keV state excited by $l=1$ stripping with a strength of 0.07. The stripping character of this transition clearly demonstrates mixing with the $2p$ orbital. No candidate for the MBZ $\frac{3}{2}^-$ state has been found in ^{47}Ti .¹⁴

As demonstrated in Fig. 4, the calculations of Malik and Scholz can successfully account for the absence of the $\frac{3}{2}^-$ state in ^{47}Ti and its presence in ^{49}V , provided that a negative deformation is assumed for ^{49}V and a positive

¹⁰ J. D. McCullen, B. F. Bayman, and L. Zamick, Phys. Rev. **134**, B515 (1965).

¹¹ F. B. Malik and W. Scholz, Phys. Rev. **150**, 919 (1966).

¹² N. Auerbach, Phys. Letters **24B**, 260 (1967).

¹³ J. Rapaport, A. Sperduto, and W. W. Buechner, Phys. Rev. **143**, 808 (1966); T. A. Belote, W. Dorenbusch, O. Hansen, and J. Rapaport, Nucl. Phys. **73**, 321 (1965).

¹⁴ Baruch Rosner and Lars Broman, Nucl. Phys. **A100**, 59 (1967).

deformation for ^{47}Ti . However, even if the known positive-parity states are omitted from the experimental level schemes, the observed level densities are still larger than those predicted by this model.

B. $T=\frac{5}{2}$ States

The isobaric analog state of the ^{49}Ti ground state should occur at 6.3–6.5-MeV excitation in ^{49}V . Since this transition carries little strength in the $(^3\text{He},d)$ reaction $[(2j+1)S=0.4]$ and is kinematically unfavored, it is not surprising that no candidate for such an assignment can be uniquely determined from among the levels of Table I. A comparison between the present data and the $^{48}\text{Ti}(d,p)^{49}\text{Ti}$ data of Ref. 7 reveals that the strong $(^3\text{He},d)$ transitions to states 76 (7783 keV) and 82 (8111 keV) may correspond to the strong $l=1$ transitions to ^{49}Ti states at 1384 and 1724 keV, respectively, observed in the (d,p) reaction. The $(^3\text{He},d)$ angular distributions are consistent with $l=1$ assignments and both transitions are among the strongest observed, as are the corresponding (d,p) transitions. The Coulomb energies corresponding to the two proposed $T=\frac{5}{2}$ states are shown in Table IV. It is characteristic that the $(^3\text{He},d)$

reaction in the energy range considered (6.4–8.7 MeV) excites, altogether, 42 states, compared to a total of eight (d,p) transitions in the corresponding ^{49}Ti range (0–2.3 MeV).

If the DW calculations are extrapolated from the bound to the unbound region, keeping the bound-state wave function fixed near zero binding, the estimated $(^3\text{He},d)$ strengths of the two $l=1$ transitions to the analog states (levels 76 and 82) are ≈ 0.4 and ≈ 0.15 , respectively. The corresponding $^{48}\text{Ti}(d,p)$ strengths divided by $(2T+1)=5$ are 0.5 and 0.12, respectively.

ACKNOWLEDGMENTS

The authors wish to thank Professor R. Middleton and Professor W. E. Stephens for their continued interest in this work. It is a pleasure to acknowledge the help of Dr. R. H. Bassel in performing part of the distorted-wave analysis, and also P. Neogy, who assisted with the data analysis. The excellent service rendered by the NEUCC computing centre in Lundtofte, Denmark is greatly appreciated. The scanning of the nuclear emulsions was carefully performed by Mrs. M. Srinivasan and Mrs. C. Coliukus.

Distribution of Radionuclides from the Interaction of 3- and 29-GeV Protons with Silver*

SEYMOUR KATCOFF, HARRY R. FICKEL,† AND ARMIN WYTENBACH‡
Chemistry Department, Brookhaven National Laboratory, Upton, New York

(Received 4 August 1967)

Formation cross sections have been measured of about 60 radionuclides isolated from Ag irradiated by 3- and 29-GeV protons. From these data, isobaric charge distributions and mass-yield curves were derived. At 3 GeV, the total isobaric cross sections are ~ 40 mb near the target, and they decrease to a broad minimum of 4 mb at around $A=30-40$. For lighter products the cross sections increase again. At 29 GeV, light- and intermediate-mass products ($20 < A < 50$) have 20–100% higher cross sections than at 3 GeV; the heavier products ($A > 65$) have 10–20% lower yields. Corresponding charge-distribution curves at the two energies are identical except for shifts in absolute magnitude. Comparison of the 3-GeV mass-yield curve with the results of a Monte Carlo calculation based on a cascade-evaporation model shows that such a mechanism can account for the observed cross sections down to about mass 50. The lower-mass products ($15 < A < 35$) must be formed mainly in a fragmentation or “fission-like” process. Comparisons are made with previous nuclear-emulsion and radiochemical results.

INTRODUCTION

NUCLEAR reactions of high-energy particles with complex nuclei have been studied by a variety of techniques.^{1,2} These involve the use of counters, nuclear

emulsions, bubble chambers, mass spectrometry, and radiochemistry. The last two methods have been used to measure product cross sections from the reaction of GeV protons with various targets.^{3–7} However, no complete

* Research performed under the auspices of the U. S. Atomic Energy Commission.

† Present address: Domtar Research Centre, Senneville, P. Q. Canada.

‡ Present address: Eidg. Institut für Reaktorforschung, Würenlingen, Switzerland.

¹ J. M. Miller and J. Hudis, *Ann. Rev. Nucl. Sci.* **9**, 159 (1959).

² J. Hudis, *High-Energy Nuclear Reactions, Nuclear Chemistry*, edited by L. Yaffe (Academic Press Inc., New York, 1967), Chap. 3.

³ R. Wolfgang, E. W. Baker, A. A. Caretto, J. B. Cumming, G. Friedlander, and J. Hudis, *Phys. Rev.* **103**, 394 (1956).

⁴ J. R. Grover, *Phys. Rev.* **126**, 1540 (1962).

⁵ G. Rudstam and G. Sørensen, *J. Inorg. Nucl. Chem.* **28**, 771 (1966).

⁶ G. Friedlander, *Physics and Chemistry of Fission* (International Atomic Energy Agency, Vienna, 1965), Vol. II, p. 265.

⁷ J. Hudis, I. Dostrovsky, G. Friedlander, J. R. Grover, N. T. Porile, L. P. Remsberg, R. W. Stoener, and S. Tanaka, *Phys. Rev.* **129**, 434 (1963).